IEICE TRANS. INF. & SYST., VOL.E98–D, NO.11 NOVEMBER 2015

PAPER

Performance of a Bayesian-Network-Model-Based BCI Using Single-Trial EEGs

Maiko SAKAMOTO[†], **Hiromi YAMAGUCHI**[††], ***Nonmembers***, **Toshimasa YAMAZAKI**[†††a)], **Ken-ichi KAMIJO**[††††], ***and*** **Takahiro YAMANOI**[†††††], ***Members***

SUMMARY We have proposed a new Bayesian network model (BNM) framework for single-trial-EEG-based Brain-Computer Interface (BCI). The BNM was constructed in the following. In order to discriminate between left and right hands to be imaged from single-trial EEGs measured during the movement imagery tasks, the BNM has the following three steps: (1) independent component analysis (ICA) for each of the single-trial EEGs; (2) equivalent current dipole source localization (ECDL) for projections of each IC on the scalp surface; (3) BNM construction using the ECDL results. The BNMs were composed of nodes and edges which correspond to the brain sites where ECDs are located, and their connections, respectively. The connections were quantified as node activities by conditional probabilities calculated by probabilistic inference in each trial. The BNM-based BCI is compared with the common spatial pattern (CSP) method. For ten healthy subjects, there was no significant difference between the two methods. Our BNM might reflect each subject's strategy for task execution.

key words: *BCI, Bayesian network, single-trial EEG, ICA, ECDL*

1. Introduction

Over the last decade, the study of complex networks has dramatically expanded across diverse scientific fields, ranging from social science to physics and biology. Especially in neuroscience, brain functional connectivity networks (BFCNs) [1] have been increasingly constructed using multi-channel electroencephalograms (EEGs) [2] and diffusion MRI [3]–[5]. However, in the former approach, because the nodes are electrode positions, they have little functional meaning. The graphical models for the latter one required large-scale anatomical data [3] and huge quantities of diffusion MRI data [4], [5].

Recently, some authors have been attempting to construct BFCN models with not so many nodes [6], [7]. Yamazaki *et al.* [6] introduced Bayesian networks (BNs) and dynamic BNs as BFCN models using EEGs. This BN construction is characterized as follows: (1) the categorical data obtained by equivalent current dipole source localization (ECDL), after independent component analysis (ICA), from single-trial EEGs [8]; (2) nodes that represent the brain sites where ECDs are located, and edges between the nodes which are weighted by the conditional probability as the brain connectivity; (3) each single-trial EEG, which is perfectly quantified by the probabilistic inference. We applied these BNs to Brain-Computer Interfaces (BCIs) with hand-movement imagery tasks. In [6], the number of single trials for the BN learning and a classification rule to discriminate among the tasks that would have been executed by subjects were determined. This study will compare the BN-model-based BCI with the existing method with the best performance [9], and investigate the characteristics of the present BNM.

Manuscript received January 20, 2015.
Manuscript revised May 30, 2015.
Manuscript publicized August 6, 2015.

[†]The author is with Hitachi Public System Service Co. Ltd., Tokyo, 136–0075 Japan.
[††]The author is with Knowledge Discovery Research Laboratories, NEC Corp., Kawasaki-shi, 211–8666 Japan.
[†††]The author is with Kyushu Institute of Technology, Iizuka-shi, 820–8502 Japan.
[††††]The author is with Medical Solutions Division, NEC Corp., Tokyo, 108–8558 Japan.
[†††††]The author is with Hokkai Gakuen University, Sapporo-shi, 064–0926 Japan.
a) E-mail: t-ymzk@bio.kyutech.ac.jp
DOI: 10.1587/transinf.2015EDP7017

2. Materials and Methods

This study was afresh approved by the ethics committees for Human Subject Researches, Faculty of Computer Science and Systems Engineering, Kyusyu Institute of Technology, and informed consent had been obtained from all subjects prior to participation.

This chapter, concerning subjects, experimental design, EEG, EOG and EMG recordings, ICA, ECDL and BN model construction, is the same as in [6]. The following is briefly summarized.

Ten healthy right-handed subjects (two females and eight males; mean age: 28.4 ± 4.27 years) participated in this experiment. Any of three kinds of line drawings of hands were presented on a monochromatic monitor of an AV tachistoscope (IS-701B, IWATSU ISEL) 0.9 m away from the subjects' eyes (Fig. 1 (a)): (1) right-hand stimulus to imagine being shaken with the subject's right hand, (2) left-hand one for the subject's left hand imagery and (3) open-right-hand one as control (Fig. 1 (b)). According to these stimuli, the subject's task is to imagine grasping the right-hand stimulus with her or his own right hand (right-hand-movement imagery: RH-MI), or to image grasping the left-hand stimulus (left-hand-movement imagery: LH-MI).

Using an electro cap (ECI, Electrocap International), EEG was recorded from 32 electrodes (FP1, FPz, FP2, F7, F3, Fz, F4, F8, FC5, FC1, FC2, FC6, T3, C3, Cz, C4, T4, CP5, CP1, CPz, CP2, CP6, T5, P3, Pz, P4, T6, PO3, POz, PO4, O1, Oz, O2) defined on the basis of the International

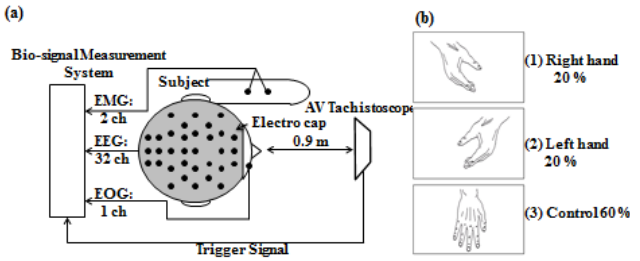

Fig. 1 Experimental design. (a) EEG, EOG and EMG recordings, and stimulus presentation. (b) Stimulus contents.

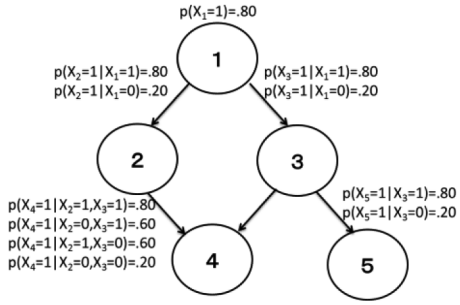

Fig. 2 An example for causal model of Bayesian network.

10-20 System [10] (Fig. 1 (a)). EOG was measured with two electrodes placed directly above the nasion and the outer canthus of the right eye. Additionally, surface EMG electrodes were placed on the common digital extensor muscles of each subject so that EEGs could be excluded when mistakenly actually grasping during the movement imagery.

The 32 signals of the EEGs were amplified by a Biotop 6R12-4 amplifier (GE Marquette Medical Systems Japan, Ltd.), and filtered a frequency bandwidth of 0.01-100 Hz. The amplified signals were sampled at a rate of 1 kHz during an epoch of 100 ms preceding and 700 ms following the stimulus onset. The inter-stimulus interval (ISI) was 1600 ms.

The 800 (=100+700)-ms epoch for the EEGs was set as follows. Bereitschaftspotential (BP) consists of early BP and the steeper negative slope (NS'), where the NS' appears about 400 ms before EMG onset [11]. Another finding [12] was that, during oddball paradigm for obtaining P300, the reaction time for button-pressing responses ranged from 357 to 505 ms after the stimulus onset. If the reaction time could be equivalent to the EMG onset, the NS' might appear −43 ms to 105 ms after the stimulus onset. Therefore, the above epoch adequately covers this interval.

The data analytical procedure in our BCI involves three steps: ICA, ECDL and BNM construction in the following.

2.1 ICA

Fast ICA [13] was applied to each of single-trial EEGs recorded during these tasks, using ICALAB [14]. Xu *et al.* [15] and Wang *et al.* [16] executed the data reduction by PCA before ICA. Here, after ICA for each trial, among 32 ICs, we removed those associated with eye movement and line noise, and having a broader high frequency (50-100 Hz) spectrum that might be likely to be generated by scalp muscles [17], according to the spectra of all the ICs for each trial. Consequently, the following ECDL was applied to 15 ICs containing only neural activity.

2.2 ECDL

Independent EEG sources obtained by ICA are dipolar [18]. ECDL was applied to the reconstructed EEGs, namely the projection of each of the rest ICs on the scalp surface by the deflation procedure, using "SynaCenterPro" (PC-based commercial software for multiple ECDL) (NEC Corporation). This software estimates unconstrained dipoles [19] at any timepoint, using the three-layered concentric sphere head model by the nonlinear optimization methods [20]. An unconstrained dipole was estimated at any timepoint with maximal peak or trough in the reconstructed EEGs for each IC. Here, we searched for appropriate and reliable dipole solutions, by selecting localization results only with goodness of fit (GOF) of more than 90% and with the simplified confidence limits (CLs) of less than 1 mm, by restricting to the results with no drastic change in the brain sites where the unconstrained dipoles are located at least twenty successive instants including the peak or trough, and by excluding the ECDL results localized to the cerebral ventricles and the corpus callosum.

We carried out anatomical labeling of the brain where ECDs were located, using the Japanese brain atlas for a single subject. The atlas includes the correspondence between three-dimensional coordinates in the brain and the anatomical labeling of the brain region. The labeling was made with reference to the textbook of neuroanatomy [21]. Each subject's MRI was transformed into the atlas, then the estimated ECDs were projected onto the atlas by this nonlinear transformation, and finally anatomical labels on the atlas were determined [22]. The picked-up different labels spread themselves over cortical and subcortical regions and the cerebellum, such as the frontal (superior, middle and inferior gyri except for Brodmann area 4 and 6), temporal, occipital and cingulate gyri, the insula, parietal association, primary motor, premotor and somatosensory cortices and the hippocampus.

2.3 Bayesian Network Model (BNM) Construction

Figure 2 shows a typical BN, showing both the topology and the conditional probability tables (CPTs), given the joint probability distribution:

$$p(X_1, \ldots, X_5|B_S) = p(X_1)p(X_2|X_1)p(X_3|X_1)p(X_4|X_1, X_3)p(X_5|X_3),$$

where X_i $(i = 1, \ldots, 5)$ (nodes) are random variables whose values could be 0 or 1, and B_S represents the BN topology, and Table 1 depicts 20 sample data generated from the BN model (BNM) [6] (originally quoted from [23]). The BN

Table 1 Data example generated by the BN shown in Fig. 1.

	node number				
	1	2	3	4	5
1	1	0	1	1	1
2	0	0	0	1	0
3	1	1	1	1	1
4	1	1	1	1	0
5	1	1	1	1	0
6	1	1	0	0	0
7	1	0	0	0	0
8	0	0	0	0	0
9	0	0	0	0	0
10	0	1	1	1	1
11	0	0	0	0	0
12	1	1	1	1	1
13	0	0	1	1	1
14	1	1	1	1	1
15	1	0	1	1	1
16	1	1	1	0	0
17	1	1	0	1	0
18	1	1	1	0	0
19	1	1	0	1	0
20	1	1	1	0	1
ave	.7	.6	.6	.6	.4

Table 2 A summary for categorized ECDL results. "L" and "R" represent the LH- and RH-MI tasks, respectively, and "IC"s independent components. "frontal", "temporal", ..., "left motor area" and "right motor area" depict the brain regions where ECDs were located for each IC. For example, red "1" at (R1, "right motor area" of 4th IC) means that 4th IC after deflation was localized to "right motor area" for the 1st trial of the RH-MI task.

		1st IC				2nd IC				4th IC			
	trials	frontal	temporal	left motor area	right motor area	frontal	temporal	left motor area	right motor area	frontal	temporal	left motor area	right motor area
L	1	0	1	0	0	1	0	0	0	1	0	0	0
	2	1	0	0	0	0	0	0	0	0	1	0	0
	⋮	⋮	⋮	⋮	⋮	⋮	⋮	⋮	⋮	⋮	⋮	⋮	⋮
	30	0	0	0	0	1	0	0	0	0	1	0	0
R	1	0	0	0	0	0	0	0	0	0	0	0	1
	2	1	0	0	0	1	0	0	0	1	0	0	0
	⋮	⋮	⋮	⋮	⋮	⋮	⋮	⋮	⋮	⋮	⋮	⋮	⋮
	30	1	0	0	0	1	0	0	0	1	0	0	0

Table 3 Results on the accuracy (in %) for the present BNM and the CSP in the validation phase. "-" means that conditional probability was not able to be calculated due to many missing values. Parentheses in "CSP" depict frequency bands used in the 1-CSP.

Subjects	BNM	CSP
1	90	75 (γ)
2	85	70 (α)
3	-	60 (γ)
4	60	70 (β)
5	65	70 (μ)
6	60	70 (γ)
7	55	65 (β,γ)
8	50	70 (γ)
9	-	70 (μ,β)
10	60	65 (β,γ)

construction refers to that the topology of BNMs is estimated from such data in Table 1. The present BNM consists of functionally distinct sites of the brain as nodes and directed relationships among these sites as edges. The nodes of the BNM are the brain sites where ECDs were located by the ECDL method. The BNM topology was decided by the conditional independency test [24]. For the brain regions (nodes) where ECDs were located, 1.0 was assigned to the conditional probability. Then, by the probabilistic inference, the conditional probability was determined for all the rest nodes. The probabilistic inference is made by the belief propagation using the clique tree algorithm [25]. The free software, "MSBNx" (Microsoft Research) [26] enables this inference, in addition to the BNM topology. The initialization in the "MSBNx" is to fix the following six items: "Forbidden links", "Root & leaf nodes", "Causes & effects", "Complete ordering", "Partial ordering" and "Advanced setting". The "Forbidden links" means no links between two specific nodes. The "Root & leaf nodes" refers to setting of root and leaf nodes. The "Causes & effects" indicates setting of nodes which are proved to affect each other in advance. The rest items were assigned to "default", as recommended by the MSBNx. The BNMs obtained for each subject had maximally fifteen nodes corresponding to the brain sites such as the frontal, temporal, occipital and cingulate gyri, hippocampus, insula, left and right parietal cortices, left and right cerebellum, left and right somatosensory areas, left and right motor areas, and others (see also Table 3). So, the "Forbidden links" were assigned to "occipital↔frontal", and the "Root and leaf nodes" to "occipital" as root. The early Bereitschaftspotential (BP) begins in the pre-supplementary motor area (preSMA) and the SMA proper and then in the premotor cortex, and the late BP (NS') occurs in the primary motor and premotor cortices [12]. Therefore, the "Causes & effects" were assigned to "frontal"→"motor area", "frontal"→"cingulate gyrus" and "cingulate gyrus"→"motor area".

Thus, each trial was characterized by the BNM as exemplified in Table 1. Hereafter, *node activities* refer to the summation of conditional probabilities at each node. Especially, by paying attention to "left and right motor areas" node activities, we proposed a rule to classify each trial into left- and right-hand imageries [6].

2.4 Learning and Validation Phases

Our BNM-based BCI consisted of learning and validation phases. In the learning phase, each about 30 trials was used for the LH- and RH-MI tasks, while the next each 10 trials in the validation phase. Especially, by paying attention to "left and right motor areas" nodes, we predicted which hand was imagined on the basis of a classification rule. This rule is that if "the left motor areas" node activities are different from "the right motor areas" ones, the trial was judged to be a right hand imagery, while if both of the node activities are the same, the trial a left hand imagery.

The CSP to be compared with our method is an algorithm for obtaining a spatial filter to transform multi-channel EEG data with two conditions into the surrogate space enabling the optimal discrimination of the conditions. This filtering is achieved by solving the generalized eigenvalue problem for the estimates of the covariance matrices of the band-pass filtered EEG signal. For each trial, 1-dimensional feature is calculated after operating the spatial filter on the single-trial EEG. From these features, the threshold is determined so that all the trials are optimally discriminated be-

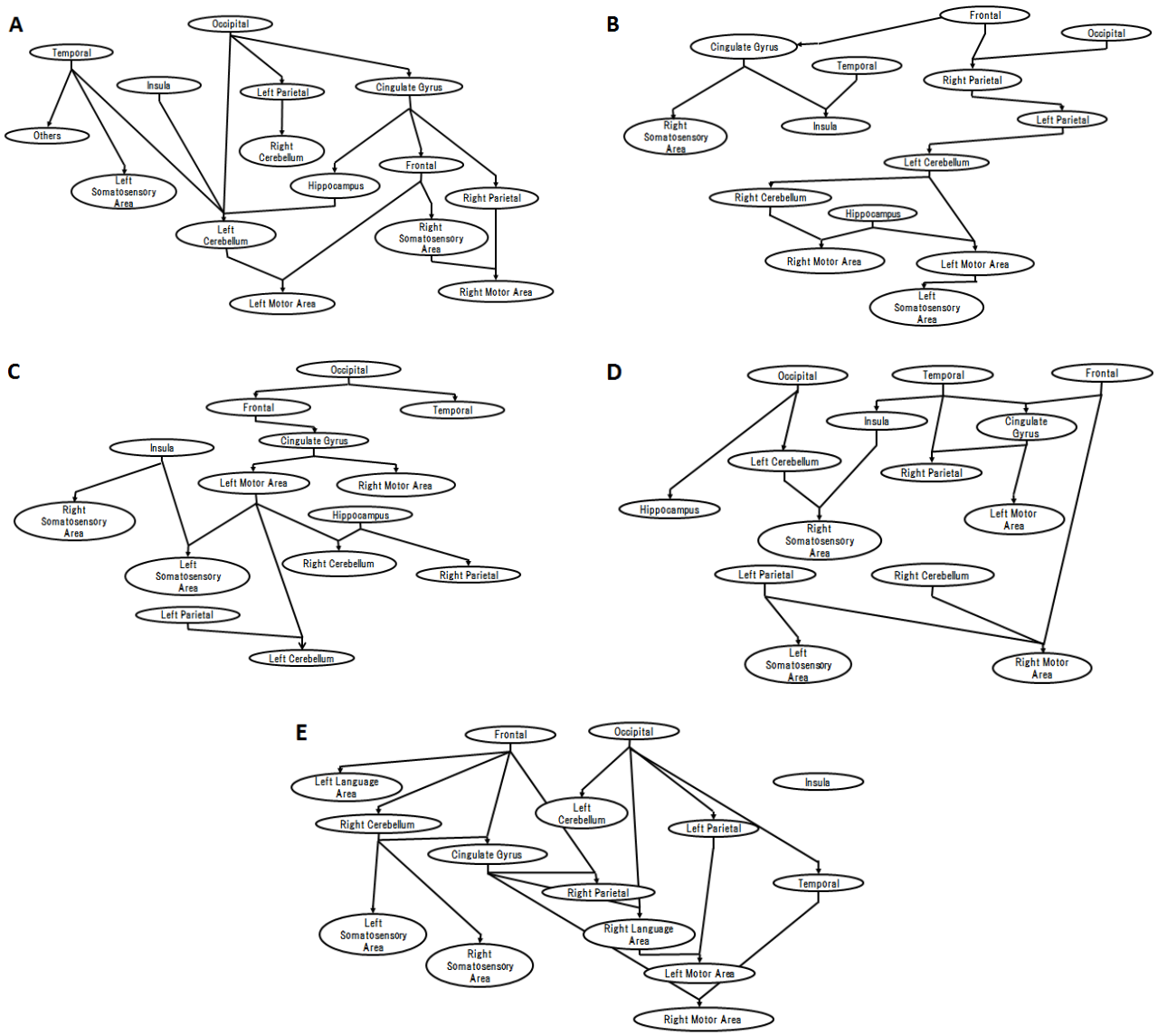

Fig. 3 BNMs for subjects 1 (A), 2 (B), 4 (C), 5 (D) and 6 (E).

tween the two conditions. Thus, for each of α, μ, β and γ frequency bands, we prepared 1-feature CSP classifier which was conducted by the same EEG data as used in the above learning phase.

2.4.1 Learning Phases

The learning phase means the BNM construction. By the 30-trial EEGs, the BNM for each subject was constructed by the ICA, the ECDL and then the probabilistic inference. Table 2 exemplifies a summary of ECDL results for one subject.

2.4.2 Validation Phases

Using another ten trials during the motor imagery task, the present BCI was validated and compared with the CSP. The EEGs during the task were analyzed by ICA and ECDL, and the ECDL results were inputted to the BNM obtained in the learning phase. Then, the node activities for all the nodes were calculated using the probabilistic inference.

3. Results

Table 3 shows the comparison of the present method and the CSP in terms of accuracy. For example, "90" in "BNM" means 18/20. There was no significant difference between the two methods ($t(16) = -0.6117$, $p > 0.10$).

4. Discussion

There was no difference between the present BNM-based BCI and the CSP-based one. Nevertheless, the BNM only for subjects 1 and 2 yielded the higher accuracy than the

CSP. However, the subjects 1, 2, 4 and 5 satisfied with the classification rule [6]. So, we attempted to attribute the difference between subjects 1 and 2 and 4 and 5 to their BN structures.

Figures 3 A-E show their BN structures. The paths to left and right "motor area" nodes go by way of "cerebellum" and/or "parietal" for subjects 1 and 2, while those for subjects 4 and 5 directly "frontal" and "cingulate gyrus". For subject 6, the path to left "motor area" goes via "language area" (including Broca's and Wernicke's areas) and "parietal", and that to right "motor area" via "temporal" and "cingulate gyrus". By introspective report, it was found that this subject silently spoke "gyu" to imagine squeezing. On the other hand, the BNM for subject 2 contains a path: "occipital"→"parietal"→"cerebellum"→"motor area" via "hippocampus". By the BN structure, one could easily guess the tasks requiring to confirm the position of the line drawing on the display, and to imagine grasping the stimulus. Thus, our BNM for each subject might reflect her or his strategy for task execution.

5. Conclusion

Motivated by the use of categorical data obtained by ECDL for EEGs after ICA, we utilized BNMs for single-trial-EEG-based BCIs, leading us to a new framework for BCIs. The compact BNM presented herein enables us easily to understand the structural and functional perspectives of the entire brain during task execution. The classification rule derived from our BNM node activities was strongly supported both by Bai *et al.* [28] for actual movement and Pfurtscheller *et al.* [29] for motor imagery. However, when applying our BNMs to motor-imagery-based BCIs, its performance would be largely determined by the classification rule. Moreover, because only subjects 1 and 2 satisfying the classification rule had the higher accuracy than the CSP, the performance might be also determined by BN structures. Thus, the BNM presented herein for each subject might reflect her or his strategy for task execution. Because this study enabled us easily to use the network for presenting the graphical models of the single-trial-EEG-based BCI data, we believe that our compact BNM does have significant potential as a BFCN.

Acknowledgments

This research was partly supported by a Grants-in-Aid for Scientific Research (B) (20300196) – The Japan Society for the Promotion of Science.

References

[1] O. Sporns, Networks of the Brain, MIT Press, London, 2011.
[2] S. Micheloyannis, E. Pachou, C.J. Stam, M. Vourkas, S. Erimaki, and V. Tsirka, "Using graph theoretical analysis of multi channel EEG to evaluate the neural efficiency hypothesis," Neuroscience Letters, vol.402, no.3, pp.273–277, 2006.
[3] C.J. Honey, R. Kötter, M. Breakspear, and O. Sporns, "Network structure of cerebral cortex shapes functional connectivity on multiple time scales," PNAS, vol.104, no.24, pp.10240–10245, 2007.
[4] P. Hagmann, M. Kurant X. Gigandet, P. Thiran, V.J. Wedeen, R. Meuli, and J.-P. Thiran, "Mapping human whole-brain structural networks with diffusion MRI," PLoS ONE, vol.7, no.7, e597, 2007.
[5] G. Gong, Y. He, L. Concha, C. Lebel, D.W. Gross, A.C. Evans, and C. Beaulieu, "Mapping anatomical connectivity patterns of human cerebral cortex using in vivo diffusion tensor imaging tractography," Cereb. Cortex, vol.19, no.3, pp.524–536, 2009.
[6] T. Yamazaki, M. Sakamoto, S. Takata, H. Yamaguchi, K. Tanaka, T. Shibata, H. Takayanagi, K. Kamijo, and T. Yamanoi, "Equivalent-current-dipole-source-localization-based BCIs with motor imagery," in Brain-Computer Interface Systems – Recent Progress and Future Prospects, ed. R. Fazel-Rezai, pp.155–174, InTech, Croatia, 2013.
[7] T. Yamazaki, R. Urata, T. Toh, and Y. Kuroiwa, "Brain functional connectivity network: theoretical basis," Neurological Medicine, vol.81, no.2, pp.204–209, 2014 (in Japanese).
[8] T. Yamazaki, K. Tanaka, T. Shibata, H. Yamaguchi, M. Ouda, Y. Sasaguri, S. Hirose, H. Takayanagi, H. Maki, T. Yamanoi, and K. Kamijo, "Categorical-data-based BCI with motor imagery using equivalent current dipole source localization," Journal of Rehabilitation Robotics, vol.1, pp.1–12, 2014.
[9] B. Blankertz, R. Tomioka, S. Lemm, M. Kawanabe, and K.-R. Müller, "Optimizing spatial filters for robust EEG single-trial analysis," IEEE Signal Proc. Magazine, vol.25, no.1, pp.41–56, 2008.
[10] L. Soufflet, M. Toussaint, R. Luthringer, J. Gressor, R. Minot, and J.P. Macher, "A statistical evaluation of the main interpolation methods applied to 3-dimensional EEG mapping," Electroencephalogr. Clin. Neurophysiol., vol.79, no.5, pp.393–402, 1991.
[11] H. Shibasaki and M. Hallett, "What is the bereitschaftspotential?," Clin. Neurophysiol, vol.117, no.11, pp.2341–2356, 2006.
[12] T. Yamazaki, K. Kamijo, A. Kenmochi, S. Fukuzumi, T. Kiyuna, Y. Takaki, and Y. Kuroiwa, "Multiple equivalent current dipole source localization of visual event-related potentials during oddball paradigm with motor response," Brain Topogr., vol.12, pp.159–175, 2000.
[13] A. Hyvärinen and E. Oja, "A fast fixed-point algorithm for independent component analysis," Neural Comput., vol.9, no.7, pp.1483–1492, 1997.
[14] A. Cichocki, S. Amari, K. Siwek, T. Tanaka, A.H. Phan, R. Zdunek, S. Cruces, P. Georgiev, Y. Washizawa, Z. Leonowicz, H. Bakardijan, T. Rutkowski, S. Choi, A. Belouchrani, A. Barros, R. Thawonmas, T. Hoya, W. Hashimoto, and Y. Terazono, "ICALAB version 3 toolbox," RIKEN BSI, http://www.bsp.brain.riken.jp/ICALAB/, 2007.
[15] N. Xu, X. Gao, B. Hong, X. Miao, S. Gao, and F. Yang, "BCI competition 2003-Data set IIb: enhancing P300 wave detection using ICA-based subspace projections for BCI applications," IEEE Trans. Biomed. Eng., vol.51, no.6, pp.1067–1072, 2004.
[16] Y. Wang, Y.T. Wang, and T.P. Jung, "Translation of EEG spatial filters from resting to motor imagery using independent component analysis," PLoS ONE, vol.7, no.5, e37665, 2012.
[17] S. Makeig, A.J. Bell, T.P. Jung, and T.J. Sejnowski, "Independent component analysis of electroencephalographic data," Adv. Neural Inform. Process. Syst., pp.145–151, 1996.
[18] A. Delorme, J. Palmer, J. Onton, R. Oostenveld, and S. Makeig, "Independent EEG sources are dipolar," PLoS ONE, vol.7, no.2, e30135, 2012.
[19] J.C. Mosher, P.S. Lewis, and R.M. Leahy, "Multiple dipole modeling and localization from spatio-temporal MEG data," IEEE Trans. Biomed. Eng., vol.39, no.6, pp.541–557, 1992.
[20] K. Kamijo, T. Kiyuna, Y. Takaki, A. Kenmochi, T. Tanigawa, and T. Yamazaki, "Integrated approach of an artificial neural network and numerical analysis to multiple equivalent current dipole source localization," Frontier Med. Biol. Eng., vol.10, no.4, pp.285–301, 2001.
[21] H.-J. Kretschmann and W. Weinrich, Klinische Neuroanatomie und kranielle Bilddiagnostik, 3rd ed., Stuttgart: Georg Thieme Verlag,

2003 (translated into Japanese).
[22] K. Tanaka, M. Motoi, Y. Sasaguri, T. Yamazaki, H. Takayanagi, T. Yamanoi, and K. Kamijo, "A new single-trial-EEG-based BCI – Validation of quantification methods of type II modeling," Clinical Neurophysiology 2010; 121 S161 (Abstracts of ICCN 2010), 29th International Congress of Clinical Neurophysiology, Oct. 28–Nov. 1, 2010, Kobe, Japan.
[23] K. Shigemasu, M. Ueno, and Y. Motomura, "Introduction to Bayesian Networks," Baifukan Co, Tokyo, Japan, 2009.
[24] J. Cheng, R. Greiner, J. Kelly, D. Bell, and W. Liu, "Learning Bayesian networks from data: an information-theory based approach," Artif. Intel., vol.137, no.1-2, pp.43–90, 2002.
[25] L. Tung, "A clique tree algorithm exploiting context specific independence," MS-thesis, University of British Columbia, 2002.
[26] C.M. Kadie, D. Hovel, and E. Horvitz, "MSBNx: A Component-Centric Toolkit for Modeling and Inference with Bayesian Networks," Technical Report, MSR-TR-2001-67, 2001.
[27] M. Hallett, J. Fieldman, L.G. Cohen, N. Sadato, and A. Pascual-Leone, "Involvement of primary motor cortex in motor imagery and mental practice," Behav. Brain Sci., vol.17, no.2, p.210, 1994.
[28] O. Bai, Z. Maria, S. Vorbacha, and M. Hallett, "Asymmetric spatiotemporal patterns of event-related desynchronization preceding voluntary sequential finger movements: a high-resolution EEG study," Clin. Neurophysiol., vol.116, no.5, pp.1213–1221, 2005.
[29] G. Pfurtscheller, C. Brunner, A. Schlogl, and F.H. Lopes da Silva, "Mu rhythm (de)synchronization and EEG single-trial classification of different motor imagery tasks," NeuroImage, vol.31, no.1, pp.153–159, 2006.

Maiko Sakamoto received a Master's degree from the Graduate School of Computer Science and System Engineering, Kyushu Institute of Technology in 2011. She is with Hitachi Public System Service Co. Ltd., Tokyo.

Hiromi Yamaguchi received BSc (IT) from Department of Bioscience and Bioinformatics, Kyushu Institute of Technology in 2013 and a Master's degree from the Graduate School of Computer Science and System Engineering, Kyushu Institute of Technology in 2015. She is currently with Knowledge Discovery Research Laboratories, NEC Corporation.

Toshimasa Yamazaki is a professor in the Department of Bioscience and Bioinformatics, Kyushu Institute of Technology. He received a bachelor of Mathematics in 1980, and the M.S. and Ph.D. in information engineering from Hokkaido University in 1982 and 1988, respectively. He was working in NEC from 1985 to 2007, and was a visiting researcher at the Netherlands Ophthalmic Research Institute from 1991 to 1992. His research interests include various BMIs using EEGs, brain functional connectivity network and Bioinformatics. He is a member of the Institute of Electronics, Information and Communication Engineers, Japanese Society of Clinical Neurophysiology and Society for Neuroscience.

Ken-ichi Kamijo is a senior manager in Medical Solutions Division, NEC Corporation. He received a bachelor of Engineering in 1984, and the M.S. and Ph.D. in information engineering from Tsukuba University, in 1986 and 2003, respectively. He was a visiting scholar at Stanford University in the US from 1993 to 1994. His research interests include bioinformatics and signal/image processing for medical systems. He is a member of the Institute of Electronics, Information and Communication Engineers and Japanese Society for Medical and Biological Engineering.

Takahiro Yamanoi is a professor in the Division of Life Science and Technology, Faculty of Engineering, Hokkai-Gakuen University. He received the M.S. and Ph.D. in information engineering from Hokkaido University in 1976 and 1982, respectively. He was a research assistant, Faculty of Engineering, Hokkaido University from 1979, a visiting researcher, Laboratory GRAI, Bordeaux University I, France from 1984, an associate Professor, Hokkai-Gakuen University from 1987, a visiting Professor, MIF, Faculty of Medicine, Aix-Marseille University II, France from 1999 to 2000, director of Admissions Section, Hokkai-Gakuen University from 2002 to 2006 and Dean of Faculty of Engineering, Hokkai-Gakuen University from 2009 to 2012. His research interests include spatiotemporal activities in the human brain and BCI. He is a member of Japan Society for Fuzzy Theory and Intelligent Informatics, The Institute of Electronics, Information and Communication Engineers, Information Processing Society of Japan and Japanese Society for Medical and Biological Engineering.